

^{17}O Solid-State NMR Spectroscopy of Lipid Membranes

Published as part of *The Journal of Physical Chemistry B virtual special issue "Charles L. Brooks III Festschrift"*.

Riqiang Fu* and Ayyalusamy Ramamoorthy*



Cite This: *J. Phys. Chem. B* 2024, 128, 3527–3537



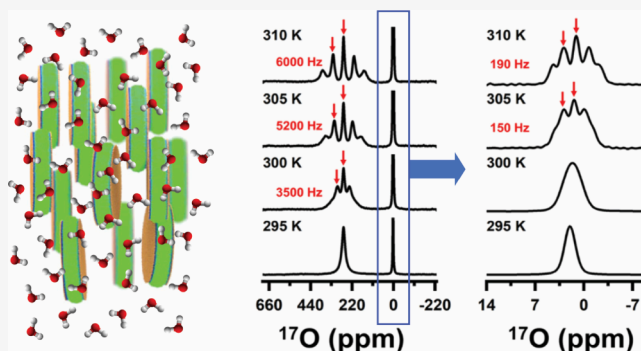
Read Online

ACCESS |

Metrics & More

Article Recommendations

ABSTRACT: Despite the limitations posed by poor sensitivity, studies have reported the unique advantages of ^{17}O based NMR spectroscopy to study systems existing in liquid, solid, or semisolid states. ^{17}O NMR studies have exploited the remarkable sensitivity of quadrupole coupling and chemical shift anisotropy tensors to the local environment in the characterization of a variety of intra- and intermolecular interactions and motion. Recent studies have considerably expanded the use of ^{17}O NMR to study dynamic intermolecular interactions associated with some of the challenging biological systems under magic angle spinning (MAS) and aligned conditions. The very fast relaxing nature of ^{17}O has been well utilized in cellular and in vivo MRS (magnetic resonance spectroscopy) and MRI (magnetic resonance imaging) applications. The main focus of this Review is to highlight the new developments in the biological solids with a detailed discussion for a few selected examples including membrane proteins and nanodiscs. In addition to the unique benefits and limitations, the remaining challenges to overcome, and the impacts of higher magnetic fields and sensitivity enhancement techniques are discussed.



INTRODUCTION

Oxygen is essential for all living organisms and is a constituent of most biological compounds and materials. Despite being highly abundant, it has not been the first choice of probe for NMR studies. This is mainly because the only NMR active isotope of oxygen, ^{17}O , is poorly abundant (0.037%) with a small gyromagnetic ratio ($\sim 1/7$ th of ^1H ; $\gamma = -3.628 \times 10^{-7} \text{ rad s}^{-1} \text{ T}^{-1}$) and therefore it has a very low NMR sensitivity. In other words, its NMR receptivity is ~ 0.1 million times lower than that of ^1H and ~ 650 times lower than that of ^{13}C . In addition, the spin-5/2 ^{17}O can exhibit very large quadrupole coupling, which can pose difficulties in obtaining narrow spectral lines unlike other rare nuclei such as ^{13}C and ^{15}N . However, experimental and theoretical developments have enabled the utilization of unique advantages of ^{17}O based NMR spectroscopy. The large chemical shift anisotropy (~ 2000 ppm) and quadrupole coupling (~ 20 MHz) have been shown to be remarkably sensitive to local environments including bonding, nonbonding, and motional interactions. As a result, ^{17}O NMR has been widely used to study inorganic materials, organic crystals, hybrid materials, and biological systems. For details on these studies, we refer the readers to published review articles.^{1–3} Although the quadrupole interaction is suppressed by the molecular motion in isotropic liquids and solutions, spectral lines are typically broad because they provide a fast relaxation mechanism. Nevertheless, the

large span of isotropic chemical shift of ^{17}O (~ 250 ppm) has been used to study systems in solution.⁴ For example, ^{17}O NMR is a valuable technique to probe protein–ligand interactions using ^{17}O -labeled small molecules and also to probe the interactions between water and macromolecules. On the other hand, the fast relaxation properties have been well utilized in the MRS (magnetic resonance spectroscopy) and MRI (magnetic resonance imaging) applications.^{5,6} Recent developments in ^{17}O NMR spectroscopy to study biological systems are summarized below.

^{17}O NMR applications to study biological systems in aqueous solution have been steadily growing since Zhu and Wu^{7,8} comprehensively analyzed the quadrupole relaxation process over the entire range of molecular motion (i.e., from $\omega_0\tau_c \ll 1$ to $\omega_0\tau_c \gg 1$, where τ_c is the rotational correlation time of the molecule under study and ω_0 is the ^{17}O Larmor frequency). It was theoretically predicted and experimentally confirmed^{7,8} that the line width for the quadrupole central transition (QCT) is narrower in the slow-motion region (i.e.,

Received: February 15, 2024

Revised: March 23, 2024

Accepted: March 25, 2024

Published: April 3, 2024



$\omega_0\tau_c \gg 1$) than in the fast-motion region (i.e., $\omega_0\tau_c \ll 1$). In addition, the relaxation process of the ^{17}O quadrupolar interaction induces the so-called dynamic frequency shift away from its true isotropic chemical shift. This dynamic frequency shift is inversely proportional to the square of the Larmor frequency. Thus, by extrapolation in a plot of signal frequency obtained at different magnetic fields versus $(\omega_0)^{-2}$, the real ^{17}O isotropic chemical shift can be obtained, provided the molecular motion falls into the slow-motion region in these fields. Although the ^{17}O relaxation process in biological macromolecules is complicated, especially when the chemical shift anisotropy provides another relaxation mechanism, ^{17}O QCT NMR is considered to be very promising and powerful. Since most biological macromolecules exhibit longer τ_c , the condition for the extreme slow-motion region (i.e., $\omega_0\tau_c \gg 1$) can be easily fulfilled at high magnetic fields as have been demonstrated in many applications.^{7,9–11}

For solid-state samples, it has been well recognized that the central transition (CT, i.e., $-1/2 \leftrightarrow +1/2$) of a half-integer quadrupolar nucleus exhibits a characteristic second-order quadrupolar line-broadening, which cannot be completely removed by magic-angle-spinning (MAS), the most commonly used high-resolution solid-state NMR technique in which samples are rotated around an axis tilted 54.74° away from the applied magnetic field direction. Direct polarization (DP) experiment allows the acquisition of ^{17}O CT MAS spectra with the characteristic second-order quadrupolar line-broadening, whose line shape analysis can be used to determine the quadrupolar coupling constant (C_Q) and the asymmetry parameter (η_Q) of the electric field gradient (EFG) at the nucleus. The double rotation (DOR) approach¹² in which two rotors are used: a small rotor containing the sample is spun inside a large outer rotor along an axis 30.56° away from the spinning axis of the outer rotor that is simultaneously spinning along the magic-angle. High-resolution ^{17}O NMR spectra can be obtained by using the DOR technique¹² that removes the second-order quadrupolar line-broadening and therefore the spectral overlap due to the second-order quadrupolar line-broadening from various ^{17}O sites present in the molecules is also avoided. The quadrupolar parameters C_Q and η_Q can be obtained through the analyses of the spinning sideband intensities.^{13,14} However, in the past few decades, researchers have been focused on the development of multidimensional experiments to separate the second-order quadrupolar line shapes through the correlation with high-resolution NMR spectra as well as other important structural information. There are two types of correlation experiments used as summarized below.

A. ^{17}O Homonuclear Correlation Experiment. High-resolution isotropic ^{17}O NMR spectral lines obtained in one dimension are correlated with their respective second-order quadrupolar line shapes in another dimension so as to separate the overlapping peaks due to the second-order quadrupolar line-broadening. Dynamic-angle spinning (DAS)¹⁵ was the first of such two-dimensional (2D) experiments where the sample rotation angle is rapidly reoriented mechanically between the two different acquisition time periods in synchronization with the radiofrequency (RF) pulses used in the 2D experiments. Since the second-order quadrupolar line shapes are scaled by the fourth Legendre polynomial with respect to the sample rotation angle, there exist two different angles, such as 37.38° and 79.19° , where the scaled second-order quadrupolar line shapes have the same size but opposite sign. As a result, as in

the standard quadrupolar-echo experiments, the second-order quadrupolar line shapes can be refocused thus rendering the high-resolution ^{17}O NMR spectra. Similar to this refocusing idea but without dynamically reorienting the rotation angles, the multiple-quantum MAS (MQMAS)^{16,17} and satellite transition MAS (STMAS)^{18,19} experiments were proposed to obtain the correlation between the high-resolution ^{17}O spectral lines and their respective second-order quadrupolar line shapes. The MQMAS method correlates the multiple-quantum transitions with the central transitions in such a way that the quadrupolar line-broadening can be refocused after evolution during the given times, while the STMAS method is to evolve the satellite transitions for a given time, forming the quadrupolar echo with the central transitions.

B. ^{17}O -X Heteronuclear Correlation (HETCOR). In this method, the ^{17}O NMR spectrum is correlated with the high-resolution spectrum of other spin-1/2 nuclei (X). So far, NMR techniques for obtaining structural and dynamic information on biomolecules have primarily utilized ^{13}C , ^{15}N , and ^1H as probes. This approach requires high enough spectral resolution achievable for the chosen spin-1/2 nuclei such that site-specific resonances can be assigned, allowing for the detection of any tiny chemical shift changes induced by secondary structures and/or by any biomolecular partners. However, site-specific resonance assignments are not easy to obtain for macromolecules in the solid state due to severely compromised spectral resolution resulting from the lack of tumbling motions. Despite extensive effort in improving spectral resolution of solids utilizing high magnetic fields, multidimensional NMR techniques, advanced spectral editing techniques, and special isotope-labeling strategies, obtaining interatomic distance restraints instead of chemical shift perturbations remains to be the primary method for characterizing the structures and dynamics of biomolecules. On the other hand, ^{17}O NMR exhibits large quadrupolar coupling constants (in the range of 4–11 MHz for biomolecules) and large chemical shift dispersions, making it sensitive to structural and dynamical changes. For instance, ^{17}O NMR is very sensitive to the subtle differences between the subunits in the dimeric gramicidin A ion channel induced by hydrogen bonding with water, which were not detectable by ^1H , ^{13}C , or ^{15}N NMR.²⁰ In addition, oxygen directly participates in many functional processes such as ion binding; thus, ^{17}O NMR can serve as a direct probe of functional sites in biomolecules. Although ^{17}O NMR studies of biomolecules began in the 1990s, success has been limited for biomolecules due to its low sensitivity and poor resolution until the solid-state NMR techniques for effective polarization transfer between ^{17}O and X (e.g., ^1H , ^{13}C , or ^{15}N) were developed, making the ^{17}O -X correlation experiments achievable.^{21–27} So far, cross-polarization (CP), dipolar-mediated heteronuclear multiple-quantum correlation (D-HMQC),²³ z-filtered transferred-echo double-resonance (ZF-TEDOR),²⁸ and dipolar refocused insensitive nuclei enhanced by polarization transfer (D-RINEPT)²⁹ methods have been available for polarization transfer between ^{17}O and $^1\text{H}/^{13}\text{C}/^{15}\text{N}$. While their transfer efficiency is generally low, several methods could be used to boost the sensitivity such as ^1H -detection and using ^{17}O as initial polarization. 2D and 3D correlation experiments involving ^{17}O have been demonstrated in small biomolecular samples.^{21,22,25,26} In particular, the $\text{O}\cdots\text{HN}$ hydrogen bonds can be characterized.^{24–26,30}

Water plays important roles in the structure, dynamics, physicochemical properties of lipids, and biological properties

of membranes. Typically, ^{31}P , ^{13}C , ^2H , and ^1H based NMR experiments are used to study membrane mimetics such as vesicles/liposomes, bicelles, and nanodiscs. ^{17}O NMR based investigation of biomolecules in hydrated lipid membranes has been rare until the report of recent studies on the use of fast exchange between free and membrane-bound water molecules in fluid lamellar phase lipid bilayers.^{20,31} ^{17}O magnetic relaxation dispersion (MRD) experiments were used to probe the dynamics of water molecules on the nanosecond time scales that are present in the binding cavity of lipid-binding proteins.^{32,33} Deuterium (spin-1 nucleus) NMR has also been used to study water dynamics in lipid bilayers by using deuterated water. Generally, the observed ^2H NMR spectra of water exhibited a much smaller quadrupolar coupling (a few kHz) than that of rigid water (~ 220 kHz), indicating that water molecules in the lipid environments are highly mobile,^{34,35} although they can be characterized as two different types: trapped water with no quadrupolar coupling and “bound” water with a small residual quadrupolar coupling. However, recent ^{17}O NMR experiments indicated that the dynamics of water molecules in a lipid environment is much slower than what had been known from molecular dynamics simulations³⁶ and fast-time scale experimental methods,³⁷ and even the rigidly bound water with a significantly large quadrupolar coupling was found in the lipid headgroup region after selectively suppressing signals from mobile water.³⁸ A list of ^{17}O NMR methods that have been developed for use under different sample conditions is given in Table 1. The main focus

Table 1. Oxygen-17 NMR Methods Used under Different Sample Conditions

Sample status	^{17}O NMR methods	Observables
in aqueous solution	Direct polarization (DP)	line width/dynamic frequency shift
in solid state	Direct polarization (DOR/MAS)	C_Q & η_Q from 2nd-order quadrupolar line shape
	DAS/MQMAS/STMAS and ^{17}O -X HETCOR, where X = ^{15}N , ^{13}C , ^1H	C_Q & η_Q from various ^{17}O sites
	^{17}O - ^1H couplings	^{17}O - ^1H hydrogen bonding
in semi solids	Direct polarization	^{17}O RQC Different water species

of this Review is to cover the recent advances in ^{17}O NMR studies of biomolecules embedded in the lipid membrane, which exist in a semisolid state under fluid lamellar phase conditions.

■ ^{17}O NMR MEASURED FROM WATER CHANNEL IN LIPID MEMBRANES

Water is crucial, both structurally and functionally, for biomolecules including proteins, nucleic acids, RNA, and cell membranes. For example, a string of hydrogen-bonded water molecules, known as a water wire, generally exists in membrane proteins that conduct water, protons, and other ions, such as in potassium channels, aquaporins, and gramicidin A (gA). Such a water wire is responsible for facilitating structural flexibility and chemistry to mediate the transport of charge and ions across membranes. A recent ^{17}O NMR study at an ultrahigh magnetic field²⁰ demonstrated that the water exchange rate between water molecules in the water wire in the gA pore is relatively

slow on the millisecond time scale, rather than what molecular dynamics results had suggested to be on the subnanosecond time scales.

Figure 1A shows the structure of the gA dimer in a liquid-crystalline lipid bilayer, and ^{17}O NMR spectra of gA oriented in hydrated lipid bilayers are shown in Figure 1B–D. The gA

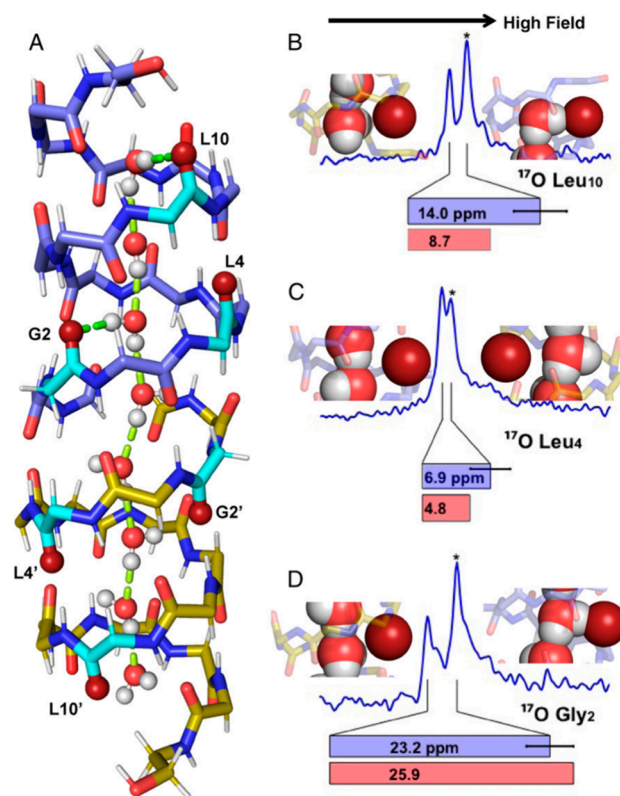


Figure 1. Oxygen-17 NMR of gramicidin A dimer in mechanically aligned liquid-crystalline lipid bilayers at 35.2 T. (A) The specific ^{17}O -labeled sites in the head-on β -helical dimeric structure of gramicidin A (gA) with a snapshot of a water wire, showing hydrogen bonding between the water wire and Leu10 and Gly2 carbonyls of the upper subunit (bright green) as well as hydrogen bonding between water molecules (pale green). Leu4 does not receive a hydrogen bond, while Leu4' appears to have a weak hydrogen bonding with water. (B–D) Observed ^{17}O NMR spectral resonances for Leu10, Leu4, and Gly2 in magnetically aligned gA obtained at 303 K with the lipid-bilayer-normal parallel to the external magnetic field direction. The G2, L4, and L10 labels in the two subunit in the gA dimer structure are distinguished with and without primes. The resonances marked (*) are shifted upfield by hydrogen bonding with water. Also shown are DFT calculations of the ^{17}O frequency shift difference between the two subunits (red bars) compared to the experimentally observed difference (blue bars). gA and dimyristoylphosphatidylcholine (DMPC) lipid were prepared via cosolubilization in trifluoroethanol at a peptide-to-lipid molar ratio of 1:16. The solution was deposited on glass slides, dried, and hydrated with 5 mM Tris buffer at pH 7.5. Stacks of 40 to 42 glass slides were incubated for >36 h at 98% relative humidity and 37 °C. The final samples contained between 42% and 48% water by weight. The proton-decoupled ^{17}O NMR spectra were acquired using a spin-echo sequence with 90° and 180° pulse lengths of 1.5 and 3.0 μs , respectively, and a 20 μs spin-echo delay period, with a 30 kHz-proton decoupling. The signal averaging time was between 3 and 6 h for each of the spectra with a recycle delay of 20 ms. ^{17}O spectra are referenced to the water signal (at 0 ppm). Figure and caption are adapted from Reference 20.

peptide was ^{17}O labeled at specific sites. Gramicidin-A, an antibiotic from *Bacillus brevis*, is a polypeptide of 15 amino acid residues having a sequence of formyl-L-Val₁-Gly₂-L-Ala₃-D-Leu₄-L-Ala₅-D-Val₆-L-Val₇-D-Val₈-L-Trp₉-D-Leu₁₀-L-Trp₁₁-D-Leu₁₂-L-Trp₁₃-D-Leu₁₄-L-Trp₁₅-ethanolamine. All of the alternating D- and L-amino acid side chains project on one side of the β -strand secondary structure, so as to force the strand to take on a helical conformation. In a lipid bilayer, the polypeptide forms a monovalent cation selective channel that is dimeric but single-stranded. The high-resolution structure of the channel monomer has been defined with 120 precise orientational constraints of ^{15}N chemical shifts, ^{15}N - ^1H dipolar couplings and ^2H quadrupolar couplings measured from solid-state NMR experiments on uniformly aligned lipid bilayer samples.^{39–41} The polypeptide backbone lines the pores wide enough to accommodate only a single file of water molecules. The outermost even-numbered carbonyl groups from Leu14, Leu12, and Leu10 in each subunit form the channel entrance and facilitate the dehydration of the cations in a stepwise process. Observing a single set of the backbone ^{15}N chemical shifts and ^{15}N - ^1H dipolar couplings from the gA sample clearly indicates the structural symmetry of the two subunits. However, for single-site ^{17}O labels (Leu14, Leu12, Leu10, Leu4, and Gly2) of the pore-lining carbonyls, each of the Leu10, Leu4, and Gly2 labels shows two well-resolved ^{17}O resonances and thus implies a break in dimer symmetry caused by the selective interactions with the water wire in the pore. As indicated in Figure 1A, the ^{17}O -Gly2 shifts are highly dependent upon the selective water hydrogen bonding strength with carbonyl oxygens. The Leu10 and Gly2 carbonyls in the upper subunit are hydrogen bonded with the water wire, while the Leu10' and Gly2' carbonyls in the lower subunit are not. Hydrogen bonding with water induces upfield shifts of the ^{17}O resonances, which highly depend on the hydrogen bonding strength between the water wire and the carbonyl oxygens, as indicated in Figure 1B–D. For the Leu14 and Leu12 residues at the pore entrance, where more water molecules are present, their ^{17}O labels show only a single resonance. However, two well-resolved ^{17}O resonances were observed in the presence of K^+ ions. For monovalent cations to pass through the pore, they must be stripped of all but two of their waters of solvation prior to entering the single file region of the pore. Owing to the acute sensitivity of the ^{17}O nucleus to its chemical environment, these ^{17}O NMR results obtained at an ultrahigh field (35.2 T) provided the direct and affirmative evidence for the first time that the selective water hydrogen bonding with carbonyl oxygens is stable on the millisecond time scale, rather than what molecular dynamics had suggested to be on the subnanosecond time scales.

■ ^{17}O NMR OF BOUND WATER OBSERVED IN HYDRATED MEMBRANES

Understanding the structure and dynamics of water molecules associated with the lipid membrane is useful to characterize various properties of the membrane and understand its capability to assist other biological processes such as protein aggregation. Many experimental and molecular dynamics simulations^{36,37} have been used to characterize water dynamics with bulk water, which is typically on the nano- to picosecond time scale. However, selectively measuring the dynamics of water molecules associated with lipid membranes has been difficult, as the bulk water molecules present in hydrated

membranes dominate the detection. SFG (sum frequency generation) experiments revealed three different types of water structures in the zwitterionic lipid–water interface:^{42–44} water strongly hydrogen-bonded to the phosphate group, water weakly hydrogen-bonded to the choline group, and water weakly interacting with carbonyl group of the lipid. Recently, Zhang et al.³⁸ developed a novel selective ^{17}O NMR technique to significantly suppress the bulk water signal, thus enabling direct detection of structured water molecules including the bound water molecules in hydrated phospholipids. Figure 2

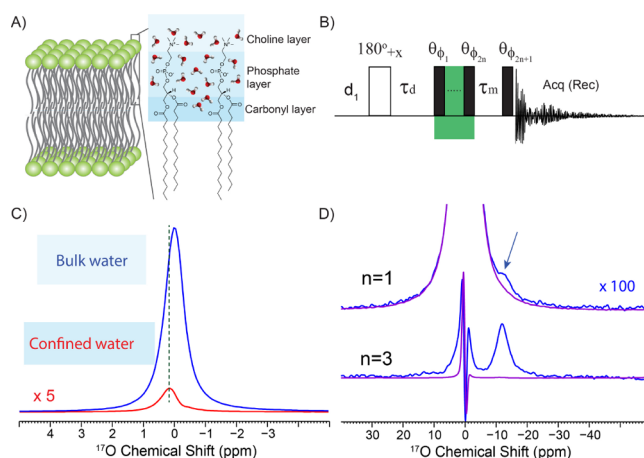


Figure 2. Observation of ^{17}O NMR spectra of different water species in hydrated dimyristoylphosphatidylcholine (DMPC) lipids. (A) Schematic model of the hydrated DMPC bilayer. The hydration of the headgroup region is highlighted with different blue background shadings, reflecting the waters that interact with the choline, phosphate, and carbonyl groups of the lipid headgroups. (B) Pulse sequence used for selectively measuring different water species. A train of pulses highlighted in green is used to selectively suppress highly mobile bulk water signals. More details on the pulse sequence and phase cycling are given in Figure 3. (C) The ^{17}O spectra taken with different inversion recovery time τ_d showing the existence of different water species with distinct chemical shifts. (D) The ^{17}O spectra using $\theta = 22.5^\circ$ (blue) and $\theta = 60^\circ$ (purple) without (top) and with (bottom) the 180° pulse. Thirty mg of powdered DMPC lipids was dissolved in 2 mL of trifluoroethanol/benzene solvent ($v/v = 1/1$). Upon flash-freezing in liquid nitrogen, the sample was placed in a vacuum chamber for 24 h to obtain a fluffy DMPC lipid powder. Thirty μL of 5 mM Tris-HCl (pH 7.5) in 80% ^{17}O enriched water was added directly to the DMPC lipid powder, and the sample tube was quickly sealed to avoid any water loss or dilution of the ^{17}O label. The sample was then allowed to equilibrate at 37°C in an incubation oven for at least 2 days, until a translucent DMPC liposome sample was formed and then packed into a 3.2 mm pencil rotor. The final hydrated DMPC liposome had a water content of $\sim 50\%$. The sample was spinning at 12 kHz. 92,160 scans were used to accumulate the signals at 303 K using Figure 2B with a recycle delay of 50 ms. Figures and captions are adapted from Reference 38.

shows a schematic model representing hydrated dimyristoylphosphatidylcholine (DMPC) lipids that may have different water molecules in the headgroup region in addition to the abundant water molecules present on the hydrophilic surface of the bilayer (cf., Figure 2A) and the ^{17}O NMR methodology for selectively measuring different water species (Figure 2B). As a result, the ^{17}O signals are dominated by highly mobile bulk water molecules, as shown in the blue spectrum of Figure 2C, such that no other water molecules associated with the lipid headgroup region can be observed. However, this

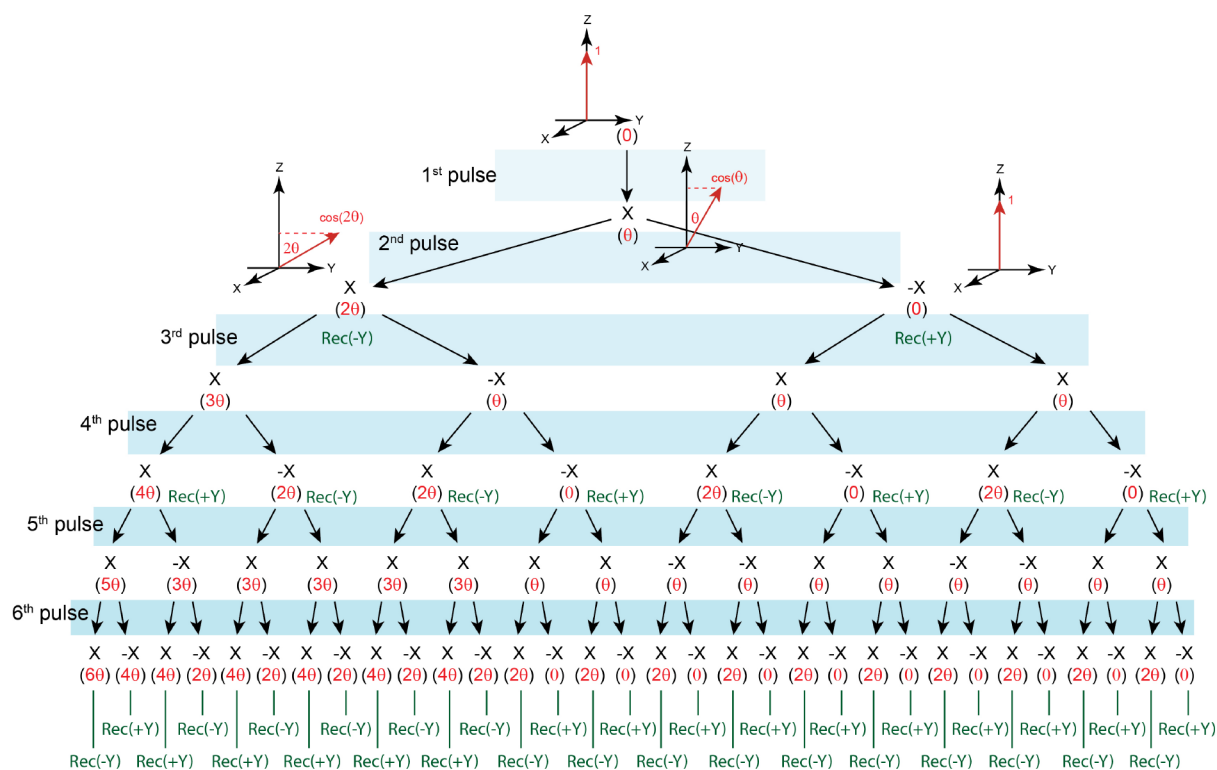


Figure 3. Design of RF phase cycling using the rotation tree under multiple RF pulses having an equal pulse length. An example of a train of pulses as highlighted in Figure 2B has been successfully used to scale down the observed signals by $S_Z = [1 - \cos(2\theta)]^n \epsilon_n$. Figure and caption are reprinted from Reference 38.

dominant water signal exhibited a much shorter ^{17}O spin-lattice relaxation time (T_1) than that of the pure water signal. Zhang et al.³⁸ concluded that this dominant ^{17}O signal represents the abundant water molecules (i.e., bulk water) whose motional freedom is greatly reduced by their fast exchange (much faster than millisecond time scale) with the water molecules present in the lipid headgroup outer layer (i.e., the choline layer in Figure 2A). This was confirmed by the ^{17}O NMR spectrum of the mechanically aligned hydrated DMPC bilayer showing a well-resolved pentet pattern with ~ 6.4 kHz residual quadrupolar coupling (RQC), similar to the observation from magnetically aligned lipid nanodisks.³¹ By setting the inversion recovery time to 2.6 ms where the dominant ^{17}O signal was zero-crossing, another ^{17}O peak was observed (the red spectrum in Figure 2C) whose chemical shift is slightly downfield by ~ 0.17 ppm and its T_1 value is shorter than the dominant ^{17}O signal. This water species is stable, and it is chemically and dynamically different from the abundant water molecules and thus likely to be located in the encapsulated pocket (i.e., the phosphate layer shown in Figure 2A) between the negatively charged phosphate and positively charged choline groups of the lipids.

A direct NMR probe of bound states in such hydrated systems has been evasive, largely because their signals are obscured by those of highly mobile and dominant free states, unless their resonances are far away from the free states.¹¹ In principle, multiple quantum filtering techniques^{45,46} can be used to suppress the signal from free water; however, they cannot efficiently excite the multiple-quantum signals, making it difficult to obtain the lowly populated water molecules that are in the bound states. Recently, a train of pulses as highlighted in Figure 2B³⁸ was proposed to effectively scale the

observed signals by $S_Z = [1 - \cos(2\theta)]^n \epsilon_n$ according to the pulse flip angle,^{38,47} as illustrated in Figure 3, where $\epsilon_n = 1, 1/2, 1/4,$ and $1/8$ for $n = 0, 1, 2,$ and 3 , respectively. Different from the multiple quantum filtering techniques, this method directly manipulates the single quantum signals based on the pulse flip angle, such that the efficiency to obtain signal from bound water is high.⁴⁷ Due to its limited flexibility, the bound water has a much stronger quadrupolar coupling as opposed to that of the mobile water. Therefore, the pulse nutation frequency to the quadrupole central transition (QCT) of the bound water is three times faster than that of a mobile water molecule. As shown in the top spectrum ($n = 1$) in Figure 2D, a very less intense QCT signal at ~ -12 ppm on the right side of the baseline of the bulk water resonance is slightly noticeable when $\theta = 22.5^\circ$ (blue spectrum, corresponding to 67.5° nutation) but completely disappears when $\theta = 60^\circ$ (purple spectrum, corresponding to 180° nutation). With a much better suppression of the bulk water signal using $n = 3$ as well as zero-crossing the bulk water signal, this QCT signal at -11.7 ppm with a line width of 4.5 ppm at half-height, whose T_1 value was measured to be an order of magnitude shorter than that of the mobile water, was clearly separated from the bulk water signal when $\theta = 22.5^\circ$ (blue spectrum) but disappeared when $\theta = 60^\circ$ (purple spectrum). Such a substantial quadrupolar coupling and a large high-field chemical shift imply that these water molecules have strong and stable hydrogen bonding. Therefore, in agreement with previously reported SFG based studies,^{42–44} these water molecules are likely to have hydrogen bonding with the fatty acyl chain ester linkages to the glycerol moiety of the lipid headgroup, as illustrated in the carbonyl layer in Figure 2A. This single extra-stable bound water in the lipid headgroup

region could be biologically, functionally, and structurally significant.

■ ^{17}O RESIDUAL QUADRUPOLE COUPLINGS MEASURED FROM ALIGNED LIPID BILAYERS

One of the powerful solid-state NMR approaches to study lipid membranes and membrane-associated peptides and proteins is the use of an aligned sample system. For example, synthetic lipid bilayers are aligned either mechanically using glass plates^{48–50} or magnetically using bicelles/nanodiscs^{51–56} to obtain high-resolution NMR spectra. Such spectra are typically used to measure the anisotropic interactions such as CSA, heteronuclear dipolar couplings and quadrupole couplings to determine atomic-resolution structure, dynamics, and membrane orientation of peptides or proteins associated with the membrane.^{57–59} This solid-state NMR approach has been successfully applied to address a number of important biological and biomedical questions. These applications include the ion-channel activities of peptides and proteins, mechanisms of membrane disruption by antimicrobial peptides and amyloid proteins/peptides, effects of lipid composition on the structure and function of P450 enzyme, and other membrane proteins, as well as protein–protein and protein–ligand complexes. In this solid-state NMR approach, ^{31}P NMR is widely used due to the use of phospholipids in the synthetic lipid bilayer system and ^{31}P nucleus is highly abundant and has a high NMR sensitivity. In addition, the naturally abundant ^{14}N present in phosphocholine lipid and ^2H from deuterated lipids are also used to measure the motionally averaged quadrupole interaction. Recent studies demonstrated the unique application of natural-abundance ^{17}O NMR to study aligned samples.^{31,60} Since water is abundantly present in the lipid bilayer samples used in NMR studies and the fast exchange between lipid-bound and free water heavily suppresses the quadrupole interaction, ^{17}O NMR has been shown to be feasible to study the aligned lipid bilayer systems.

Figure 4 displays natural-abundance ^{17}O NMR spectra of water present in a SMA-QA polymer based lipid nanodiscs sample.³¹ The nanodisc contains a DMPC lipid bilayer encased by synthetic amphipathic polymer as illustrated in Figure 4A. The size (~ 25 nm diameter) and homogeneity of the nanodiscs are revealed by the TEM image, as shown in Figure 4B. The ^{17}O NMR spectra exhibit an isotropic peak for temperatures below the gel-to-liquid crystalline phase transition of the DMPC lipids in the nanodiscs indicating the isotropic nature of nanodiscs that average out the ^{17}O quadrupole interaction (Figure 4D, see the spectrum at 295 K). As the temperature of the sample is increased well above T_m , the magnetic alignment of nanodiscs exhibits anisotropic ^{17}O quadrupole interaction arising from the lipid-bilayer-bound water molecules, while their exchange with free bulk water molecules reduces the observed quadrupole interaction. As a result, a pentet pattern is observed for the five transitions in the spin- $S/2$ ^{17}O above T_{mm} , i.e., the spectra obtained at 310 and 315 K. The isotropic peak observed well below T_{mm} (i.e., at 295 K) becomes broader as observed at 300 and 305 K as the lipids are undergoing the phase transition while the polymers present on the belt of the nanodiscs broaden the phase transition temperature, indicating the loss of cooperativity in melting. As demonstrated by the observed spectra from samples containing different concentrations of nanodiscs (Figure 4C), a high concentration (30% w/v) is required to

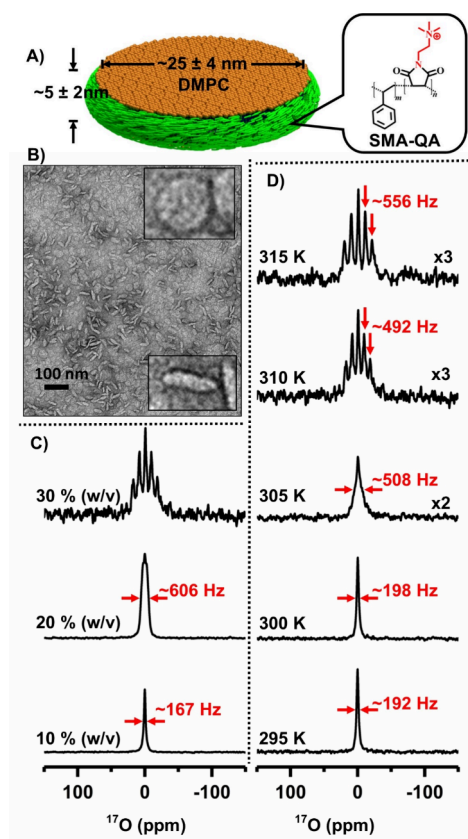


Figure 4. Natural-abundance ^{17}O NMR spectra of magnetically aligned polymer nanodiscs. (A) Schematic representation of SMA-QA polymer based lipid nanodiscs. (B) Transmission electron microscopy image of SMA-QA:DMPC (0.5:1 w/w) nanodiscs. ^{17}O NMR spectra of water from SMA-QA:DMPC (0.5:1 w/w) nanodiscs (~ 25 nm diameter) for varying lipid concentrations at 310 K (C) and at the indicated temperatures for 30% w/v lipid concentration (D). SMA-QA (styrene maleic acid quaternary ammonium) is a positively charged amphipathic polymer that has been demonstrated to form nanodiscs and to isolate membrane proteins directly from cell membrane. The size of the nanodisc can be varied by varying the polymer:lipid ratio. The synthetic polymer is typically characterized by mass spectrometry and ^{13}C CPMAS solid-state NMR. Nanodiscs are purified by using size exclusion chromatography (SEC) to remove free polymer and lipid aggregates. The size of the nanodiscs is typically determined by dynamic light scattering (DLS), and TEM images and ^{31}P solid-state NMR experiments are also used to characterize the nanodiscs. NMR spectra were obtained from 400.11 MHz NMR spectrometer (54.24 MHz for ^{17}O nuclei) using a Hahn-echo pulse sequence with $12 \mu\text{s}$ 90° pulse, $20 \mu\text{s}$ echo delay, 0.2 s relaxation/recycle delay, 400 ppm spectral width, and 0.2 s acquisition time. Depending on the sample amount used in the experiment, the number of scans used to acquire the reported ^{17}O NMR spectra were varied between 10,000 and 20,000 to obtain a reasonable signal-to-noise ratio. All other details on the sample preparation, characterization, and experimental conditions can be found in Reference 31. Figure and caption are reprinted from Reference 31.

overcome the complete averaging of ^{17}O quadrupole interaction by the tumbling motion of the nanodiscs. As shown in Figure 5, the 90° flipping of the alignment axis of nanodiscs, i.e., flipping the lipid-bilayer-normal from orthogonal to parallel direction to the external magnetic field, changed the observed ^{31}P anisotropic chemical shift (from -13.6 ± 0.5 to $\sim 22.7 \pm 3.7$ ppm) and ^{14}N RQC (from $\sim 8.9 \pm 0.6$ to $\sim 16.8 \pm 0.7$ kHz) according to the second-order

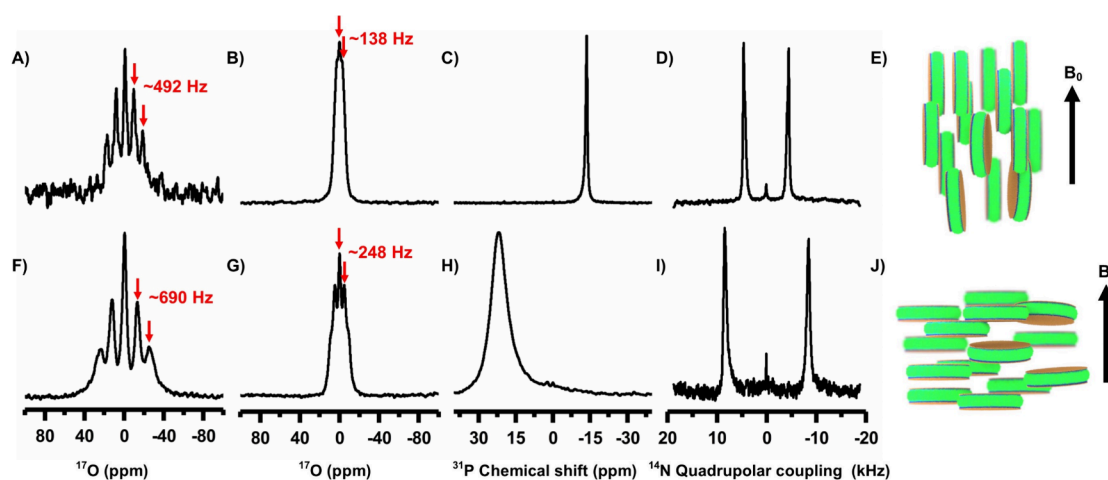


Figure 5. NMR spectra of magnetically aligned and flipped nanodiscs. ^{17}O (A, B, F, and G), ^{31}P (C and H), and ^{14}N (D and I) NMR spectra of magnetically aligned SMA-QA:DMPC nanodiscs obtained at 310 K with the lipid-bilayer-normal perpendicular (top row, as illustrated in E) and parallel (bottom row, as illustrated in J) to the external magnetic field direction. A 2 mM YbCl_3 solution was used to flip the nanodiscs (bottom row). All spectra were acquired from 20% w/v lipid concentration, except that 30% w/v was used for A and F. All other details on the sample preparation, characterization, and experimental conditions can be found in Reference 31. Figure and caption are adapted from Reference 31.

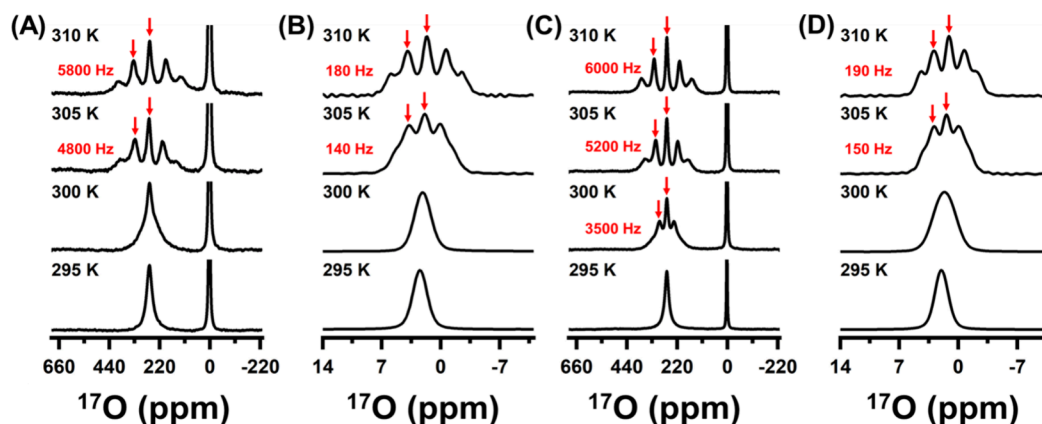


Figure 6. Oxygen-17 NMR spectra of 30 mM benzoic acid with 1:1 INPEN:DMPC, 25% DMPC nanodiscs collected at (A, B) 14.1 T and (C, D) 18.8 T. The spectra in (A, C) display the full spectral widths, and the spectra in (B, D) are zoomed in to show the line shape of the water peak. Figure and caption are adopted from Reference 60 with permission.

polynomial function ($3 \cos^2 \theta - 1$), with θ being the angle between the magnetic field axis and lipid-bilayer-normal. On the other hand, the observed ^{17}O RQCs did not follow the above-mentioned trend and indicated that the motional averaging is different in flipped and unflipped nanodiscs. This observation suggests that ^{17}O RQCs could be useful in investigating the dynamic molecular events occurring at the membrane surface.

MAGNETICALLY ALIGNED NANODISCS TO MEASURE ^{17}O RQCS FROM SMALL MOLECULE

An alignment medium is commonly used in high-throughput NMR based structural studies to measure motionally averaged anisotropic NMR parameters such as residual dipolar couplings (RDCs) and residual chemical shift anisotropies (RCSAs). Recent studies have demonstrated the use of magnetically aligned nanodiscs as a new alignment medium in the structural studies of proteins, RNA, and small molecules. Interestingly, a recent study demonstrated the feasibility of using aligned nanodiscs to measure ^{17}O RQCs from a small molecule.^{61–63}

Figure 6 demonstrates the use of nanodiscs to measure ^{17}O RQCs from ^{17}O -labeled benzoic acid.⁶⁰ A combination of

nonionic INPEN based amphipathic polymer and DMPC lipids is used to prepare nanodiscs containing ^{17}O -labeled benzoic acid. As mentioned above, the nanodiscs magnetically align with the lipid-bilayer-normal perpendicular to the external magnetic field direction well above the main phase transition temperature of the constituted lipids. For example, the ^{17}O NMR spectra recorded at 310 K display two different pentet patterns well separated by the significantly different chemical shift values arising from ^{17}O nuclei associated with water and benzoic acid molecules. As mentioned above, the fast exchange between lipid-bound and free water molecules significantly averages the ^{17}O quadrupole couplings, resulting in a very narrow pentet pattern with much smaller RQCs (~ 180 Hz) as compared to that from benzoic acid molecules, which exhibit about 33 times larger RQC (~ 6000 Hz). This study also compared the ^{17}O NMR spectra obtained from 400 and 800 MHz NMR spectrometers to demonstrate the advantage of using a higher magnetic field to obtain enhanced sensitivity and resolution.

This successful demonstration of the feasibility of measuring ^{17}O RQCs from small molecules using flipped and unflipped magnetically aligned nanodiscs opens avenues for structural

studies of a variety of small molecules including pharmaceutical compounds and their polymorphs that may not be crystallizable for structure determination by X-ray crystallography.

UNIQUE ADVANTAGES OF HIGH MAGNETIC FIELDS FOR ^{17}O NMR SPECTROSCOPY

Recent developments in NMR instrumentation and higher magnetic fields have created new avenues for the development and applications of solid-state NMR spectroscopy.^{64–69} Particularly, the high magnetic fields are well suited for studies using ^{17}O based NMR spectroscopy. In addition to the better sensitivity, resolution, and enhanced magnetic alignment, higher magnetic fields can also be used to probe water induced changes in the observed NMR parameters as demonstrated in Figure 1. ^{17}O NMR spectra of aligned lipid bilayers containing gA obtained at 35.2 T are shown in Figure 1. It should be recognized that the ^{17}O shifts shown in Figure 1B,D represent the anisotropic chemical shift of the carbonyl oxygens of gA oriented in lipid bilayers with the bilayer-normal parallel to the applied magnetic field. These observed anisotropic ^{17}O shifts could be resulting either from the reorientations of the electron cloud or from the changes in the electron cloud induced by hydrogen bonding with the water wire. From ^{17}O MAS spectra in Figure 7, the Gly2 site shows

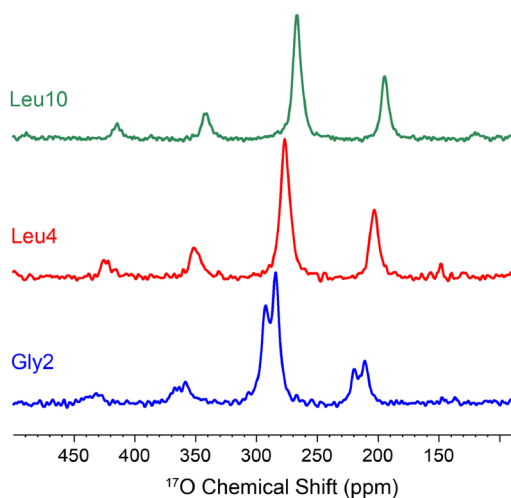


Figure 7. Oxygen-17 MAS NMR spectra of selectively ^{17}O -labeled gA embedded in hydrated DMPC lipid bilayers acquired at a 35.2 T magnetic field (unpublished). 100,000 scans were accumulated at 303 K for each spectrum with a recycle delay of 50 ms using triple pulses.⁴⁷ The sample conditions were the same as those indicated in Figure 1.

two isotropic resonances, clearly indicating that hydrogen bonding with water changes the density of the electron cloud. On the other hand, the other sites (Leu4 and Leu10) show a single isotropic resonance, suggesting the hydrogen bonding with water only reorients the electron cloud. The combination of static solid-state NMR experiments on magnetically aligned bilayers (as shown in Figure 1) and MAS experiments (as shown in Figure 7) can be useful to obtain structural insights around the labeled ^{17}O site in terms of how the electron cloud changes upon hydrogen bonding with the water wire in the gA channel.

SUMMARY AND FUTURE DIRECTIONS

Understanding biomolecular activities at atomic resolution is crucial to describing their functions. Significant advances in instrumentation and experiments have resulted in a library of NMR techniques that can be used to study dynamic structures of biomolecules in vitro, in cell, and in vivo conditions. Recent studies have shown the benefits of utilizing even the uncommon ^{17}O nuclei that pose many limitations for NMR studies despite the high abundance of oxygen atoms. In this Review, we have presented some of the benefits of ^{17}O NMR spectroscopy to study lipid membranes. The ability to observe different types of water molecules in membranes and the feasibility of differentiation of the environment in ion channels by ^{17}O NMR experiments are unique and exciting. The use of nanodiscs to measure residual ^{17}O quadrupole couplings to study the structure and dynamics of membrane-bound water and to study the phase transition of encased lipids opens new avenues in membrane biophysics.^{70–77} The fact that water plays a crucial role in biology and the advent of higher magnetic fields and better NMR instrumentations renders more sophisticated NMR techniques, the benefits of ^{17}O based NMR applications can be expected to grow remarkably. Therefore, we conclude that much remains to be done to fully utilize the power of ^{17}O based NMR spectroscopy to study biological solids.

In the past several decades, many ^{17}O based solid-state NMR techniques have been developed for studies on biomolecules, both in aqueous solution and in the solid state.³ So far, solid-state $^1\text{H}/^{13}\text{C}/^{15}\text{N}$ NMR techniques have been instrumental in advancing the structural biology of biomolecules. Due to the large ^{17}O quadrupolar couplings and chemical shift dispersions, incorporating ^{17}O NMR is expected to provide a powerful and indispensable tool for structural studies.^{21–27} However, one of the major obstacles in using ^{17}O NMR as one of the routine structural tools is the inefficient and expensive ^{17}O -enrichment of biomolecules. Labeling strategies have fortunately been improved recently.⁷⁸ On the other hand, ^{17}O solid-state NMR studies of biomolecules in the semisolid states (i.e., lipid membranes), as presented in this Review, have just begun to emerge, where ^{17}O labeling appears to be less demanding due to the presence of small molecules and water itself, as opposed to ^{17}O labeling in large biomolecules. For instance, with a simple addition of ^{17}O -labeled water into hydrated lipid environments, free and bound water molecules can be characterized by ^{17}O solid-state NMR methods.³⁸ That said, the use of site-specifically ^{17}O -labeled membrane-associated proteins or peptides can provide profound insights into their structure, dynamics, and topology; additionally, it enables the measurement of their interactions with lipids and ligands present in the sample. Since nanodiscs are increasingly utilized in the structural studies of biomolecules, protein aggregation, and drug delivery, the development of ^{17}O -labeled nanodisc-forming polymers would be valuable to probe the interaction of the reconstituted proteins with the belt of the nanodiscs.^{79–89}

Dynamic nuclear polarization (DNP), which can dramatically enhance the sensitivity of ^{17}O ,⁹⁰ makes studies of natural-abundance ^{17}O in various applications possible.^{91–93} The perspectives/potential of utilizing DNP-enhanced ^{17}O NMR in the structural biology of biomolecules are immense, but hurdles remain to be overcome, such as the assignment of ^{17}O resonances. The large ^{17}O quadrupolar couplings render the

second-order quadrupolar line-broadening, significantly compromising the ^{17}O resolution even at 800 MHz, the current limit for DNP. ^{17}O correlation experiments with other spin-1/2 nuclei can aid in the assignment of ^{17}O spectra, but the experimental sensitivity is highly dependent on ^{17}O isotope labeling. Therefore, developing high field DNP systems is crucial for the highly sensitive ^{17}O NMR studies of large biomolecules.

AUTHOR INFORMATION

Corresponding Authors

Riqiang Fu – National High Magnetic Field Laboratory, Florida State University, Tallahassee, Florida 32310, United States; orcid.org/0000-0003-0075-0410; Email: rfu@magnet.fsu.edu

Ayyalusamy Ramamoorthy – National High Magnetic Field Laboratory, Florida State University, Tallahassee, Florida 32310, United States; Department of Chemical and Biomedical Engineering, Institute of Molecular Biophysics, Florida State University, Tallahassee, Florida 32310, United States; orcid.org/0000-0003-1964-1900; Email: aramamoorthy@fsu.edu

Complete contact information is available at:
<https://pubs.acs.org/10.1021/acs.jpcc.4c01016>

Notes

The authors declare the following competing financial interest(s): The polymers used in Figures 4, 5 and 6 were produced in the Ramamoorthy lab and are US patented.

Biographies

Riqiang Fu received his B.S. degree in Electrical Engineering from the University of Science and Technology of China (USTC) and his PhD degree at Wuhan Institute of Physics (Chinese Academy of Sciences) and worked at Bruker Spectrospin (Switzerland). He then joined the research group of Professor Geoffrey Bodenhausen as a postdoctoral fellow at the University of Lausanne (Switzerland) and National High Magnetic Field Laboratory (Tallahassee, Florida). Currently he is a Research Faculty III at NHMFL. He specializes in solid-state NMR methodology development and NMR applications in materials science and biological systems.

Ayyalusamy Ramamoorthy is a professor of Chemical and Biomedical Engineering, and National High Magnetic Field Laboratory, at Florida State University. He joined FSU after obtaining his PhD in Chemistry from the Indian Institute of Technology (Kanpur, India), working in the Central Leather Research Institute (Chennai, India) and JEOL Ltd. (Tokyo, Japan), completing postdoctoral training at the University of Pennsylvania (Philadelphia), and serving at the University of Michigan (Ann Arbor) as the Robert W. Parry Collegiate Professor of Chemistry and Biophysics. He is an elected Fellow of the Royal Society of Chemistry, American Association for the Advancement of Science, ISMAR, and Michigan Society of Fellows. His current research focuses on protein aggregation and biocondensation, membrane protein structural biophysics, and applications of solid-state NMR spectroscopy.

ACKNOWLEDGMENTS

Research in the Ramamoorthy lab is supported with funding from the NIH (Grant R35GM139573 to A.R.). The NMR experiments were carried out at the National High Magnetic Field Lab (NHMFL) supported by the NSF Cooperative Agreement DMR-2128556 and the State of Florida and

supported in part by the National Resource for Advanced NMR Technology, which is funded by NIH RM1-GM148766.

REFERENCES

- (1) Lemaitre, V.; Smith, M. E.; Watts, A. A review of oxygen-17 solid-state NMR of organic materials - towards biological applications. *Solid State Nucl. Magn. Reson.* **2004**, *26*, 215–235.
- (2) Chen, J. C.; Wang, F.; Wen, Y. J.; Tang, W. P.; Peng, L. M. Emerging Applications of ^{17}O Solid-State NMR Spectroscopy for Catalytic Oxides. *ACS Catal.* **2023**, *13*, 3485–3500.
- (3) Wu, G. ^{17}O NMR studies of organic and biological molecules in aqueous solution and in the solid state. *Prog. Nucl. Magn. Reson. Spectrosc.* **2019**, *114–115*, 135–191.
- (4) Muniyappan, S.; Lin, Y. X.; Lee, Y.-H.; Kim, J. H. ^{17}O NMR Spectroscopy: A Novel Probe for Characterizing Protein Structure and Folding. *Biology* **2021**, *10*, 453.
- (5) Zhu, X. H.; Chen, W. *In vivo* ^{17}O MRS imaging - Quantitative assessment of regional oxygen consumption and perfusion rates in living brain. *Anal. Biochem.* **2017**, *529*, 171–178.
- (6) Paech, D.; Nagel, A. M.; Schultheiss, M. N.; Umatham, R.; Regnery, S.; Scherer, M.; Wick, A.; Platt, T.; Wick, W.; Bendszus, M.; et al. Quantitative Dynamic Oxygen-17 MRI at 7.0 T for the Cerebral Oxygen Metabolism in Glioma. *Radiology* **2020**, *295*, 181–189.
- (7) Zhu, J.; Wu, G. Quadrupole central transition ^{17}O NMR spectroscopy of biological macromolecules in aqueous solution. *J. Am. Chem. Soc.* **2011**, *133*, 920–932.
- (8) Zhu, J.; Ye, E.; Tersikh, V.; Wu, G. Experimental verification of the theory of nuclear quadrupole relaxation in liquids over the entire range of, molecular tumbling motion. *J. Phys. Chem. Lett.* **2011**, *2*, 1020–1023.
- (9) Zhu, J.; Kwan, I. C. M.; Wu, G. Quadrupole-central-transition ^{17}O NMR spectroscopy of protein-ligand complexes in solution. *J. Am. Chem. Soc.* **2009**, *131*, 14206–14207.
- (10) Gan, Z.; Hung, I.; Wang, X.; Paulino, J.; Wu, G.; Litvak, I. M.; Gor'kov, P.; Brey, W. W.; Lendi, P.; Schiano, J. L.; et al. NMR spectroscopy up to 35.2 T using a series-connected hybrid magnet. *J. Magn. Reson.* **2017**, *284*, 125–136.
- (11) Young, R. P.; Caulkins, B. G.; Borchardt, D.; Bulloch, D. N.; Larive, C. K.; Dunn, M. F.; Mueller, L. J. Solution-state ^{17}O quadrupole central-transition NMR spectroscopy in the active site of tryptophan synthase. *Angew. Chem., Int. Ed.* **2016**, *55*, 1350–1354.
- (12) Samoson, A.; Lippmaa, E.; Pines, A. High Resolution Solid-State NMR Averaging of Second-order Effects by Means of a double-rotor. *Mol. Phys.* **1988**, *65* (4), 1013–1018.
- (13) Sun, B.Q.; Baltisberger, J.H.; Wu, Y.; Samoson, A.; Pines, A. Sidebands in dynamic angle spinning (DAS) and double rotation (DOR) NMR. *Solid State Nucl. Magn. Reson.* **1992**, *1*, 267–295.
- (14) Engelhardt, G.; Kentgens, A.P.M.; Koller, H.; Samoson, A. Strategies for extracting NMR parameters from ^{23}Na MAS, DOR and MQMAS spectra. A case study for $\text{Na}_4\text{P}_2\text{O}_7$. *Solid State Nucl. Magn. Reson.* **1999**, *15*, 171–180.
- (15) Mueller, K. T.; Chingas, G. C.; Pines, A. NMR probe for dynamic-angle spinning. *Rev. Sci. Instrum.* **1991**, *62*, 1445–1452.
- (16) Medek, A.; Harwood, J. S.; Frydman, L. Multiple-Quantum magic angle spinning NMR: A new method for study of quadrupolar nuclei in solids. *J. Am. Chem. Soc.* **1995**, *117*, 12779–12787.
- (17) Frydman, L.; Harwood, J. S. Isotropic spectra of half-integer Quadrupolar spins from bidimensional magic-angle spinning NMR. *J. Am. Chem. Soc.* **1995**, *117*, 5367–5368.
- (18) Gan, Z. Isotropic NMR spectra of half-integer quadrupolar nuclei using satellite transitions and magic-angle spinning. *J. Am. Chem. Soc.* **2000**, *122*, 3242–3243.
- (19) Hung, I.; Gan, Z. Low-power STMAS - breaking through the limit of large quadrupolar interactions in high-resolution solid-state NMR spectroscopy. *Phys. Chem. Chem. Phys.* **2020**, *22*, 21119–21123.
- (20) Paulino, J.; Yi, M.; Hung, I.; Gan, Z.; Wang, X.; Chekmenev, E. Y.; Zhou, H. X.; Cross, T. A. Functional Stability of Water Wire-

Carbonyl Interactions in an Ion Channel. *Proc. Natl. Acad. Sci. U.S.A.* **2020**, *117*, 11908–11915.

(21) Lin, B.; Hung, I.; Gan, Z.; Chien, P.-H.; Spencer, H. L.; Smith, S. P.; Wu, G. ^{17}O NMR studies of yeast ubiquitin in aqueous solution and in the solid state. *ChemBioChem* **2021**, *22*, 826–829.

(22) Keeler, E. G.; Michaelis, V. K.; Colvin, M. T.; Hung, I.; Gor'kov, P.; Cross, T. A.; Gan, Z.; Griffin, R. G. ^{17}O MAS NMR Correlation Spectroscopy at High Magnetic Fields. *J. Am. Chem. Soc.* **2017**, *139*, 17953–17963.

(23) Hung, I.; Uldry, A. C.; Becker-Baldus, J.; Webber, A. L.; Wong, A.; Smith, M. E.; Joyce, S. A.; Yates, J. R.; Pickard, C. J.; Dupree, R.; et al. Probing Heteronuclear ^{15}N - ^{17}O and ^{13}C - ^{17}O Connectivities and Proximities by Solid-State NMR Spectroscopy. *J. Am. Chem. Soc.* **2009**, *131*, 1820–1834.

(24) Vogt, F. G.; Yin, H.; Forcino, R. G.; Wu, L. ^{17}O solid-state NMR as a sensitive probe of hydrogen bonding in crystalline and amorphous solid forms of diflunisal. *Mol. Pharmaceutics* **2013**, *10*, 3433–3446.

(25) Hung, I.; Mao, W. P.; Keeler, E. G.; Griffin, R. G.; Gor'kov, P.; Gan, Z. Characterization of peptide O...HN hydrogen bonds via ^1H -detected $^{15}\text{N}/^{17}\text{O}$ solid-state NMR spectroscopy. *Chem. Commun.* **2023**, *59*, 3111–3113.

(26) Carnahan, S. L.; Lampkin, B. J.; Naik, P.; Hanrahan, M. P.; Slowing, I. I.; VanVeller, B.; Wu, G.; Rossini, A. J. Probing O-H bonding through proton detected ^1H - ^{17}O double resonance solid-state NMR spectroscopy. *J. Am. Chem. Soc.* **2019**, *141*, 441–450.

(27) Venkatesh, A.; Hanrahan, M. P.; Rossini, A. J. Proton detection of MAS solid-state NMR spectra of half-integer quadrupolar nuclei. *Solid State Nucl. Magn. Reson.* **2017**, *84*, 171–181.

(28) Jaroniec, C. P.; Filip, C.; Griffin, R. G. 3D TEDOR NMR Experiments for Simultaneous Measurement of Multiple Carbon-Nitrogen Distances in Uniformly ^{13}C , ^{15}N -Labeled Solids. *J. Am. Chem. Soc.* **2002**, *124*, 10728–10742.

(29) Trebosc, J.; Hu, B.; Amoureux, J. P.; Gan, Z. Through-space R^3 -HETCOR experiments between spin-1/2 and half-integer quadrupolar nuclei in solid-state NMR. *J. Magn. Reson.* **2007**, *186*, 220–227.

(30) Brinkmann, A.; Kentgens, A. P. M. Proton-Selective ^{17}O - ^1H Distance Measurements in Fast Magic-Angle-Spinning Solid-State NMR Spectroscopy for the Determination of Hydrogen Bond Lengths. *J. Am. Chem. Soc.* **2006**, *128*, 14758–14759.

(31) Ravula, T.; Sahoo, B. R.; Dai, X.; Ramamoorthy, A. Natural-abundance ^{17}O NMR spectroscopy of magnetically aligned lipid nanodiscs. *Chem. Commun.* **2020**, *56*, 9998–10001.

(32) Modig, K.; Liepinsh, E.; Otting, O.; Halle, B. Dynamics of Protein and Peptide Hydration. *J. Am. Chem. Soc.* **2004**, *126*, 102–114.

(33) Modig, K.; Rademacher, M.; Lucke, C.; Halle, B. Water Dynamics in the Large Cavity of Three Lipid-binding Proteins Monitored by ^{17}O Magnetic Relaxation Dispersion. *J. Mol. Biol.* **2003**, *332*, 965–977.

(34) Volke, F.; Eisenblatter, S.; Galle, J.; Klose, G. Dynamic properties of water at phosphatidylcholine lipid bilayer surfaces as seen by deuterium and pulsed field gradient proton NMR. *Chem. Phys. Lipids* **1994**, *70*, 121–131.

(35) Faure, C.; Bonakdar, L.; Dufourc, E. J. Determination of DMPC hydration in the L_α and L_β phases by ^2H solid state NMR of D_2O . *FEBS Lett.* **1997**, *405*, 263–266.

(36) Shen, H.; Wu, Z.; Zou, X. Interfacial Water Structure at Zwitterionic Membrane/Water Interface: The Importance of Interactions between Water and Lipid Carbonyl Groups. *ACS Omega* **2020**, *5*, 18080–18090.

(37) Watanabe, N.; Suga, K.; Umakoshi, H. Functional Hydration Behavior: Interrelation between Hydration and Molecular Properties at Lipid Membrane Interfaces. *J. Chem.* **2019**, *2019*, 1–15.

(38) Zhang, R.; Cross, T. A.; Peng, X.; Fu, R. Surprising Rigidity of Functionally Important Water Molecules Buried in the Lipid Headgroup Region. *J. Am. Chem. Soc.* **2022**, *144*, 7881–7888.

(39) Ketchem, R.; Hu, W.; Cross, T. A. High-resolution conformation of gramicidin A in a lipid bilayer by solid-state NMR. *Science* **1993**, *261*, 1457–1460.

(40) Ketchem, R.; Roux, B.; Cross, T. High-resolution polypeptide structure in a lamellar phase lipid environment from solid state NMR derived orientational constraints. *Structure* **1997**, *5*, 1655–1669.

(41) Kovacs, F.; Quine, J. R.; Cross, T. A. Validation of the single-stranded channel conformation of gramicidin A by solid-state NMR. *Proc. Natl. Acad. Sci. U.S.A.* **1999**, *96*, 7910–7915.

(42) Mondal, J. A.; Nihonyanagi, S.; Yamaguchi, S.; Tahara, T. Three distinct water structures at a zwitterionic lipid/water interface revealed by heterodyne-detected vibrational sum frequency generation. *J. Am. Chem. Soc.* **2012**, *134* (18), 7842–7850.

(43) Ohto, T.; Backus, E. H. G.; Hsieh, C.-S.; Sulpizi, M.; Bonn, M.; Nagata, Y. Lipid Carbonyl Groups Terminate the Hydrogen Bond Network of Membrane-Bound Water. *J. Phys. Chem. Lett.* **2015**, *6* (22), 4499–4503.

(44) Ishiyama, T.; Terada, S.; Morita, A. Hydrogen-Bonding Structure at Zwitterionic Lipid/Water Interface. *J. Phys. Chem. Lett.* **2016**, *7*, 216–220.

(45) Navon, G.; Shinar, H.; Eliav, U.; Seo, Y. Multiquantum filters and order in tissues. *NMR Biomed* **2001**, *14*, 112–132.

(46) Shinar, H.; Eliav, U.; Navon, G. Deuterium double quantum-filtered NMR studies of peripheral and optic nerves. *Magn. Reson. Mater. Phys.* **2021**, *34*, 889–902.

(47) Wang, F. F.; Ramakrishna, S. K.; Sun, P. C.; Fu, R. Triple-pulse excitation: An efficient way for suppressing background signals and eliminating radio-frequency acoustic ringing in direct polarization NMR experiments. *J. Magn. Reson.* **2021**, *332*, 107067.

(48) Bechinger, B.; Kim, Y.; Chirlian, L. E.; Gesell, J.; Neumann, J. M.; Montal, M.; Tomich, J.; Zasloff, M.; Opella, S. J. Orientations of amphipathic helical peptides in membrane bilayers determined by solid-state NMR spectroscopy. *J. Biomol. NMR* **1991**, *1*, 167–173.

(49) Moll, I. F.; Cross, T. A. Optimizing and characterizing alignment of oriented lipid bilayers containing gramicidin D. *Biophys. J.* **1990**, *57*, 351–362.

(50) Hallock, K. J.; Henzler Wildman, K.; Lee, D.-K.; Ramamoorthy, A. An Innovative Procedure Using a Sublimable Solid to Align Lipid Bilayers for Solid-State NMR Studies. *Biophys. J.* **2002**, *82*, 2499–2503.

(51) Sanders, C. R.; Hare, B. J.; Howard, K. P.; Prestegard, J. H. Magnetically-Oriented Phospholipid Micelles as a Tool for the Study of Membrane-Associated Molecules. *Prog. NMR Spectrosc.* **1994**, *26*, 421–444.

(52) Durr, U. H. N.; Gildenberg, M.; Ramamoorthy, A. The Magic of Bicelles Lights Up Membrane Protein Structure. *Chem. Rev.* **2012**, *112*, 6054–6074.

(53) Durr, U. H. N.; Soong, R.; Ramamoorthy, A. When detergent meets bilayer: Birth and coming of age of lipid bicelles. *Prog. NMR Spectrosc.* **2013**, *69*, 1–22.

(54) Diller, A.; Loudet, C.; Aussenac, F.; Raffard, G.; Fournier, S.; Laguerre, M.; Grelard, A.; Opella, S. J.; Marassi, F. M.; Dufourc, E. J. Bicelles: A natural 'molecular goniometer' for structural, dynamical and topological studies of molecules in membranes. *Biochimie* **2009**, *91*, 744–751.

(55) Ravula, T.; Ramadugu, S. K.; Di Mauro, G.; Ramamoorthy, A. Bioinspired, Size-Tunable Self-Assembly of Polymer-Lipid Bilayer Nanodiscs. *Angew. Chem., Int. Ed.* **2017**, *56*, 11466–11470.

(56) Radoicic, J.; Park, S. H.; Opella, S. J. Macrodiscs Comprising SMALPs for Oriented Sample Solid-State NMR Spectroscopy of Membrane Proteins. *Biophys. J.* **2018**, *115*, 22–25.

(57) Opella, S. J.; Marassi, F. M. Applications of NMR to membrane proteins. *Arch. Biochem. Biophys.* **2017**, *628*, 92–101.

(58) Cross, T. A. YidC: Evaluating the Importance of the Native Environment. *Structure* **2018**, *26*, 2–4.

(59) Ahuja, S.; Jahr, N.; Im, S. C.; Vivekanandan, S.; Popovych, N.; Clair, S. V. L.; Huang, R.; Soong, R.; Xu, J.; Yamamoto, K.; et al. A model of the membrane-bound cytochrome b5-cytochrome P450

- complex from NMR and mutagenesis data. *J. Biol. Chem.* **2013**, *288*, 22080–22095.
- (60) McCalpin, S. D.; Fu, R.; Ravula, T.; Wu, G.; Ramamoorthy, A. Magnetically aligned nanodiscs enable direct measurement of ^{17}O residual quadrupolar coupling for small molecules. *J. Magn. Reson.* **2023**, *346*, 107341.
- (61) Ravula, T.; Hardin, N. Z.; Ramamoorthy, A. Polymer nanodiscs: Advantages and limitations. *Chem. Phys. Lipids* **2019**, *219*, 45–49.
- (62) Ravula, T.; Ramamoorthy, A. Measurement of Residual Dipolar Couplings Using Magnetically Aligned and Flipped Nanodiscs. *Langmuir* **2022**, *38*, 244–252.
- (63) Krishnarjuna, B.; Ravula, T.; Faison, E. M.; Tonelli, M.; Zhang, Q.; Ramamoorthy, A. Polymer-Nanodiscs as a Novel Alignment Medium for High-Resolution NMR-Based Structural Studies of Nucleic Acids. *Biomolecules* **2022**, *12*, 1628.
- (64) Reif, B.; Ashbrook, S. E.; Emsley, L.; Hong, M. Solid-state NMR spectroscopy. *Nat. Rev. Methods Primers* **2021**, *1*, 2.
- (65) Nishiyama, Y.; Hou, G.; Agarwal, V.; Su, Y. C.; Ramamoorthy, A. Ultrafast Magic Angle Spinning Solid-State NMR Spectroscopy: Advances in Methodology and Applications. *Chem. Rev.* **2023**, *123*, 918–988.
- (66) Ahlawat, S.; Mote, K. R.; Lakomek, N. A.; Agarwal, V. Solid-State NMR: Methods for Biological Solids. *Chem. Rev.* **2022**, *122*, 9643–9737.
- (67) Chow, W. Y.; De Paepe, G.; Hediger, S. Biomolecular and Biological Applications of Solid-State NMR with Dynamic Nuclear Polarization Enhancement. *Chem. Rev.* **2022**, *122*, 9795–9847.
- (68) Shcherbakov, A. A.; Medeiros-Silva, J.; Tran, N.; Gelenter, M. D.; Hong, M. From Angstroms to Nanometers: Measuring Interatomic Distances by Solid-State NMR. *Chem. Rev.* **2022**, *122*, 9848–9879.
- (69) Biedenbander, T.; Aladin, V.; Saeidpour, S.; Corzilius, B. Dynamic Nuclear Polarization for Sensitivity Enhancement in Biomolecular Solid-State NMR. *Chem. Rev.* **2022**, *122*, 9738–9794.
- (70) Ulsan, S.; Sheraj, I.; Stehling, S.; Ivanov, I.; Das, A.; Kuhn, H.; Banerjee, S. Structural and functional evaluation mammalian and plant lipoxygenases upon association with nanodiscs as membrane mimetics. *Biophys. Chem.* **2022**, *288*, 106855.
- (71) Won, J.; Kim, J. S.; Jeong, H.; Kim, J. Y.; Feng, S.; Jeong, B.; Kwak, M.; Ko, J.; Im, W.; So, I.; et al. Molecular architecture of the Ga_3 -bound TRPC5 ion channel. *Nat. Commun.* **2023**, *14*, 2550.
- (72) Harant, K.; Cajka, T.; Angelisova, P.; Pokorna, J.; Horejsi, V. Composition of raft-like cell membrane microdomains resistant to styrene-maleic acid copolymer (SMA) solubilization. *Biophys. Chem.* **2023**, *296*, 106989.
- (73) Amengual, J.; Notaro-Roberts, L.; Nieh, M. P. Morphological control and modern applications of bicelles. *Biophys. Chem.* **2023**, *302*, 107094.
- (74) Chen, L.; Yu, C. Y.; Xu, W. T.; Xiong, Y.; Cheng, P.; Lin, Z.; Zhang, Z. H.; Knoedler, L.; Panayi, A. C.; Knoedler, S.; et al. Dual-Targeted Nanodiscs Revealing the Cross-Talk between Osteogenic Differentiation of Mesenchymal Stem Cells and Macrophages. *ACS Nano* **2023**, *17*, 3153–3167.
- (75) Shimizu, C.; Ikeda, K.; Nakao, H.; Nakano, M. Amphipathic peptide-phospholipid nanofibers: Kinetics of fiber formation and molecular transfer between assemblies. *Biophys. Chem.* **2023**, *296*, 106985.
- (76) Dallo, S.; Shin, J.; Zhang, S.; Ren, Q.; Bao, H. Designer Nanodiscs to Probe and Reprogram Membrane Biology in Synapses. *J. Mol. Biol.* **2023**, *435*, 167757.
- (77) Sahoo, B. R.; Ramamoorthy, A. Direct interaction between the transmembrane helices stabilize cytochrome P450 2B4 and cytochrome b5 redox complex. *Biophys. Chem.* **2023**, *301*, 107092.
- (78) Spackova, J.; Goldberga, L.; Yadav, R.; Cazals, G.; Lebrun, A.; Verdier, P.; Metro, T. X.; Laurencin, D. Fast and cost-efficient ^{17}O -isotopic labeling of carboxylic groups in biomolecules: from free amino acids to peptide chains. *Chem.—Eur. J.* **2023**, *29*, e202203014.
- (79) Chen, H.; Ahmed, S.; Zhao, H.; Elghobashi-Meinhardt, N.; Dai, Y. X.; Kim, J. H.; McDonald, J. G.; Li, X. C.; Lee, C. H. Structural and functional insights into Spns2-mediated transport of sphingosine-1-phosphate. *Cell* **2023**, *186*, 2644–2655.e16.
- (80) Baccouch, R.; Rascol, E.; Stoklosa, K.; Alves, I. D. The role of the lipid environment in the activity of G protein coupled receptors. *Biophys. Chem.* **2022**, *285*, 106794.
- (81) Zhang, C.; Li, Q. R.; Shan, J.; Xing, J. H.; Liu, X. Y.; Ma, Y.; Qian, H. S.; Chen, X. L.; Wang, X. W.; Wu, L. M.; et al. Multifunctional two-dimensional Bi_2Se_3 nanodiscs for anti-inflammatory therapy of inflammatory bowel diseases. *Acta Biomater.* **2023**, *160*, 252–264.
- (82) Sahoo, B. R.; Genjo, T.; Bekier, M.; Cox, S. J.; Stoddard, A. K.; Ivanova, M.; Yasuhara, K.; Fierke, C. A.; Wang, Y. Z.; Ramamoorthy, A. Alzheimer's amyloid-beta intermediates generated using polymer-nanodiscs. *Chem. Commun. (Camb)* **2018**, *54*, 12883–12886.
- (83) Sahoo, B. R.; Genjo, T.; Moharana, K. C.; Ramamoorthy, A. Self-Assembly of Polymer-Encased Lipid Nanodiscs and Membrane Protein Reconstitution. *J. Phys. Chem. B* **2019**, *123*, 4562–4570.
- (84) Sahoo, B. R.; Genjo, T.; Cox, S. J.; Stoddard, A. K.; Anantharamaiah, G. M.; Fierke, C.; Ramamoorthy, A. Nanodisc-Forming Scaffold Protein Promoted Retardation of Amyloid-Beta Aggregation. *J. Mol. Biol.* **2018**, *430*, 4230–4244.
- (85) Barnaba, C.; Sahoo, B. R.; Ravula, T.; Medina-Meza, I. G.; Im, S. C.; Anantharamaiah, G. M.; Waskell, L.; Ramamoorthy, A. Cytochrome-P450-Induced Ordering of Microsomal Membranes Modulates Affinity for Drugs. *Angew. Chem., Int. Ed.* **2018**, *57*, 3391–3395.
- (86) Krishnarjuna, B.; Ravula, T.; Faison, E. M.; Tonelli, M.; Zhang, Q.; Ramamoorthy, A. Polymer-Nanodiscs as a Novel Alignment Medium for High-Resolution NMR-Based Structural Studies of Nucleic Acids. *Biomolecules* **2022**, *12*, 1628.
- (87) Krishnarjuna, B.; Im, S. C.; Ravula, T.; Marte, J.; Auchus, R. J.; Ramamoorthy, A. Non-Ionic Inulin-Based Polymer Nanodiscs Enable Functional Reconstitution of a Redox Complex Composed of Oppositely Charged CYP450 and CPR in a Lipid Bilayer Membrane. *Anal. Chem.* **2022**, *94*, 11908–11915.
- (88) Krishnarjuna, B.; Marte, J.; Ravula, T.; Ramamoorthy, A. Enhancing the stability and homogeneity of non-ionic polymer nanodiscs by tuning electrostatic interactions. *J. Colloid Interface Sci.* **2023**, *634*, 887–896.
- (89) Janata, M.; Gupta, S.; Cadova, E.; Angelisova, P.; Krishnarjuna, B.; Ramamoorthy, A.; Horejsi, V.; Raus, V. Sulfonated polystyrenes: pH and Mg^{2+} -insensitive amphiphilic copolymers for detergent-free membrane protein isolation. *Eur. Polym. J.* **2023**, *198*, 112412.
- (90) Michaelis, V. K.; Corzilius, B.; Smith, A. A.; Griffin, R. G. Dynamic Nuclear Polarization of ^{17}O : Direct Polarization. *J. Phys. Chem. B* **2013**, *117*, 14894–14906.
- (91) Perras, F. A.; Chaudhary, U.; Slowing, I. I.; Pruski, M. Probing Surface Hydrogen Bonding and Dynamics by Natural Abundance, Multidimensional, ^{17}O DNP-MAS Spectroscopy. *J. Phys. Chem. C* **2016**, *120*, 11535–11544.
- (92) Carnevale, D.; Mouchaham, G.; Wang, S.; Baudin, M.; Serre, C.; Bodenhausen, G.; Abergel, D. Natural abundance oxygen-17 solid-state NMR of metal organic frameworks enhanced by dynamic nuclear polarization. *Phys. Chem. Chem. Phys.* **2021**, *23*, 2245–2251.
- (93) Kobayashi, T.; Pruski, M. Indirectly Detected DNP-Enhanced ^{17}O NMR Spectroscopy: Observation of Non-Protonated Near-Surface Oxygen at Naturally Abundant Silica and Silica-Alumina. *ChemPhysChem* **2021**, *22*, 1441–1445.